Electrospun cerium nitrate/polymer composite fibres: synthesis, characterization and fibre-division model*

Li Meng-Meng (李蒙蒙)[a], Long Yun-Ze(龙云泽)[a]†,
Yin Hong-Xing(尹红星)[a], and Zhang Zhi-Ming(张志明)[b]

[a] *College of Physics Science, Qingdao University, Qingdao* 266071, *China*
[b] *College of Chemistry and Chemical Engineering, Ocean University of China, Qingdao* 266100, *China*

(Received 13 June 2010; revised manuscript received 18 December 2010)

Cerium (III) nitrate/poly(vinylpyrrolidone) ($Ce(NO_3)_3$/PVP) composite fibres have been prepared by electrospinning. After calcining the composite fibres in air at 500 °C, CeO_2 nanowires were obtained. The characterizations of the as-spun composite fibres and resultant nanowires have been carried out by a scanning electron microscope (SEM), an infrared spectrometer, an x-ray diffractometer and a fluorescence spectrophotometer. Interestingly, some unusual ribbon-like or twin fibres were observed besides the common fibres with circular or elliptic cross sections. We developed a fibre-division model resulting from Coulomb repulsion and solvent vaporization to interpret the formation of the ribbons or twin fibres, which has been confirmed by the SEM studies. Our results also indicate that the formation of the ribbons or twin fibres is less dependent on operation voltage and work distance.

Keywords: cerium, nanowires, electrospinning, fibre-division model

PACS: 81.07.–b, 81.05.Lg, 82.35.Np **DOI:** 10.1088/1674-1056/20/4/048101

1. Introduction

Cerium dioxide or ceria (CeO_2) is one of the cheapest and most abundant rare earth oxides, and it has received much attention due to its unique properties. It has various applications in areas such as optical devices,[1,2] microelectronic devices,[3] high storage capacitor devices[4] and polishing materials.[5] Besides those applications, several novel phenomena or properties including lattice expansion,[6] transition from boundary diffusion to lattice diffusion,[7] and blue shift in ultraviolet absorption spectra[8] have been observed in materials based on nanosized CeO_2. Various techniques have been developed for the preparation of CeO_2 nanostructures, such as the hydrothermal method,[5] sonochemical and microwave assisted heating methods,[9] and electrospinning.[10]

Electrospinning is well known as a simple, versatile and useful technology for fabricating fibres with diameters ranging from several micrometers down to 100 nm or even a few nanometers under the action of electric field forces.[11] In a traditional process of electrospinning, a Taylor cone formed under an applied high voltage and the charged solution jets ejected from the cone is rushed to a collector. At the same time, most of the solvent evaporates away. The electrospun fibres are then commonly deposited as a nonwoven web on a grounded collector.[11−15] Numerous polymer-based nanofibres, as well as metal, ceramic and glass nanofibres have been prepared by electrospinning, and their potential applications in optoelectronics, sensors, catalysis, textiles, filters, fibre reinforcement, tissue engineering, drug delivery, wound healing, etc. have been extensively explored (see Refs. [11] and [16]–[19]).

A broad range of fibre architectures is available from electrospinning, such as thin smooth fibres, beaded fibres, porous fibres, ribbon-like fibres, branched fibres and fibres with fractal surface structures, and have been reported in Ref. [16]. Among them, electrospun fibres with circular or elliptic cross sections are most commonly observed. In addition, fibres in the form of ribbons with various cross-sectional shapes are also widely observed from a number of different kinds of polymers and solvents.[16,17,20−29] For example, Huang *et al.*[20] reported on the ribbon-like fibres of a synthetic polypeptide with elastin-like properties. Good studies on spun flat polymer ribbons from 30 wt% polystyrene in dimethylformamide, 10 wt% poly(ether imide) in hexafluoro-2-propanol,

*Project supported by the Program for New Century Excellent Talents at the University of China (Grant No. NCET-07-0472) and the National Natural Science Foundation of China (Grant Nos. 11074138, 10910101081 and 10604038).

†Corresponding author. E-mail: yunze.long@163.com

© 2011 Chinese Physical Society and IOP Publishing Ltd

and 20 wt% poly(2-hydroxyethyl methacrylate) in ethanol were presented by Koombhongse *et al.*[21] They proposed that the collapsed tube-like skin led to the creation of ribbon-like fibres. Ribbon-like carbon fibres via electrospinning from pitch precursor[22,23] and ribbon-like nanofibres of barium titanate[24] were also prepared. Although ribbon-like fibres have been reported by several research groups, the mechanism of formation of ribbon-shaped fibre has not been fully discussed and understood yet.

In this paper, cerium nitrate/polymer composite fibres are fabricated by electrospinning and CeO_2 nanowires are obtained by calcining the composite fibres in air at 500 °C. Their morphological, structural and fluorescent properties are also studied. Interestingly, we also observe some unusual fibres, ribbon-like twin fibres, besides common fibres with circular or elliptic cross sections. Herein, based on our experimental results, we develop a fibre-division model to interpret the formation of these ribbon-like fibres.

2. Experimental section

2.1. Preparation of precursor solution

All the chemicals used were of analytical grade. The polymer solution was prepared by dissolving 4 g of poly(vinylpyrrolidone) (PVP, $M_W \approx 10000$) in 8 g of ethanol and then stirred thoroughly for 2 h at room temperature. Meanwhile, 0.1 g of cerium (III) nitrate ($Ce(NO_3)_3{\cdot}6H_2O$) was fully dissolved in 4 g of ethanol. Subsequently, this $Ce(NO_3)_3$ ethanol solution was added into the polymer solution and stirred thoroughly for 2 h. The resulting solution was kept at room temperature for 1 h, then the $Ce(NO_3)_3$/PVP precursor solution with 0.47 wt% $Ce(NO_3)_3$ was obtained. $Ce(NO_3)_3$/PVP solutions each with 0.92 wt% and 1.38 wt% $Ce(NO_3)_3$ were prepared in a similar way.

2.2. Preparation of composite fibres and CeO_2 nanowires

The electrospinning setup was similar to that shown in Fig. 1. A 10-ml plastic syringe with a flattened stainless steel needle (inner diameter 0.72 mm and outer diameter 1.08 mm), was fixed perpendicularly. The anode of a high-voltage dc supply was connected to the needle, and the cathode was connected to the grounded collector, a piece of aluminum foil. The applied high voltage was 10 kV–30 kV. The distance between needle tip and collector (defined as work distance) was 10 cm–20 cm. The electrospinning experiments were carried out at room temperature.

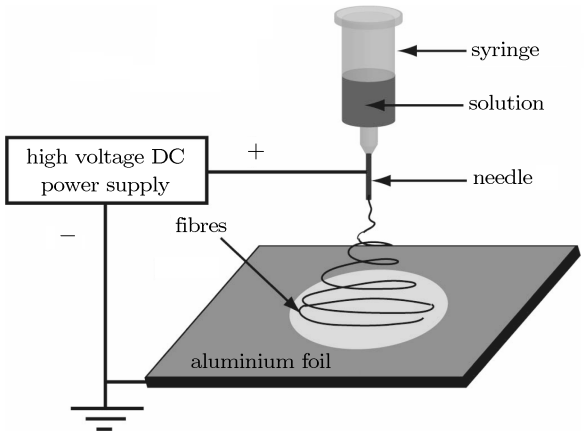


Fig. 1. Schematic of the setup for electrospinning.

In order to obtain the nanosized CeO_2, part of composite fibres were calcined in air at 500 °C with a heating rate of 5 °C/min for 3 h.

2.3. Characterization

The morphologies of the composite fibre mats and the resulting CeO_2 nanowires were characterized by a scanning electron microscope (SEM; JEOL JSM-6390). All samples were coated with an evaporated gold thin film before SEM imaging to ensure a higher conductivity. The SEM was operated at an accelerating voltage of 20 kV. Infrared (IR) spectra of the electrospun composite fibres were recorded through a MAGNA-IR 550 spectrometer. Composite fibres and CeO_2 nanowires were characterized by a Rigaku D/max-2400 x-ray diffractometer (Cu K_α radiation, $\lambda = 1.5406$ nm) with a scanning rate of 0.02°/s in 2θ ranging from 5° to 80°. In addition, the fluorescence emission spectra were measured by a HITACHI F-4600 fluorescence spectrophotometer at room temperature.

3. Results and discussion

3.1. Electrospun cerium nitrate/polymer composite fibres

$Ce(NO_3)_3$/PVP composite fibres with different amounts of $Ce(NO_3)_3$ were electrospun under the following experimental parameters: voltage 20 kV, and work distance 15 cm. From Figs. 2(a)–2(c), we can see that the composite fibres deposited on the collector are randomly oriented in the form of non-woven mats.

Additionally, some ribbon-like twin fibres are also observed in these figures. After statistical calculation, we obtain size distributions of composite fibres, as shown in Figs. 2(d)–2(f). The average diameters for fibres with 0.47 wt%, 0.92 wt%, and 1.38 wt% $Ce(NO_3)_3$ are approximately 650, 1450, and 2100 nm, respectively. It is noted that the morphology of electrospun fibre depends strongly on the $Ce(NO_3)_3$ content. Figure 2(g) exhibits $Ce(NO_3)_3$ content dependence of average diameter of composite fibre. It is indicated that the average diameter of composite fibres is nearly linear with respect to $Ce(NO_3)_3$ content, and their diameter distribution also becomes wider gradually with the increase of the $Ce(NO_3)_3$ loading.

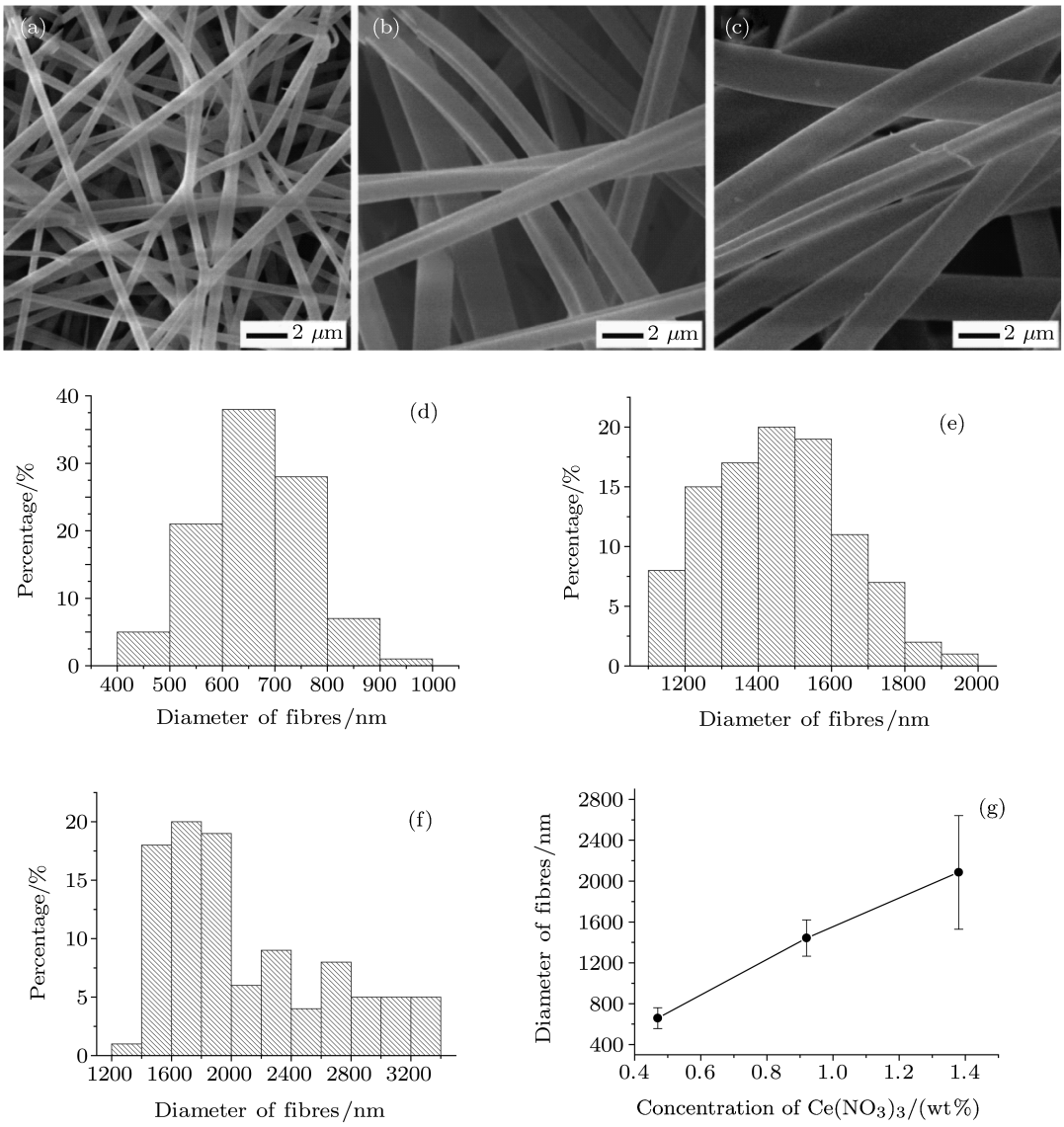


Fig. 2. (a)–(c) SEM images of electrospun $Ce(NO_3)_3$/PVP composite fibres with 0.47 wt%, 0.92 wt% and 1.38 wt% $Ce(NO_3)_3$, respectively. (d)–(f) The size distributions of panels (a)–(c) respectively. (g) $Ce(NO_3)_3$ content dependence of average diameter of composite fibres. The size distribution was obtained from 100 as-spun fibres in the SEM images. Experimental parameters are: voltage 20 kV, work distance 15 cm.

Infrared (IR) spectra of the different samples are shown in Fig. 3. The electrospun composite fibres contain trace a carboxyl group and hydroxyl group due to the precursor solutions. The sharp peak at 1680 cm^{-1} is assigned to the stretching vibration of carboxyl group, which is the typical mode of PVP.[30] A broad stretching band around 3460 cm^{-1} appears, corresponding to the vibration of the associated hydroxyl groups. The band in a range of 2850 cm^{-1}–3000 cm^{-1} can be attributed to the C–H stretching vibrations.

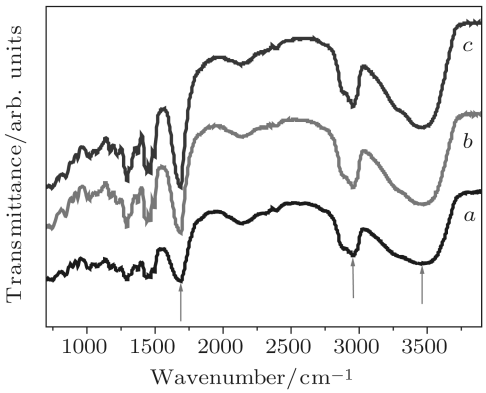


Fig. 3. IR spectra of $Ce(NO_3)_3$/PVP composite fibres with curve *a* 0.47 wt%, curve *b* 0.92 wt%, and curve *c* 1.38 wt% $Ce(NO_3)_3$.

There are no significant differences among the three IR spectra, indicating that $Ce(NO_3)_3$ content has little influence on the IR spectra.

3.2. CeO_2 nanostructures after calcinations

In order to synthesize inorganic nanostructures, electrospun $Ce(NO_3)_3$/PVP composite fibres were calcined at 500 °C for 3 h. It can be seen from Fig. 4 that nanowires each with a diameter of about 200 nm were obtained. The XRD patterns of $Ce(NO_3)_3$/PVP composite fibres and the resulting CeO_2 nanowires are presented in Fig. 5. From curve *a*, two broad peaks can be ascribed to the scattering from PVP chains at interplanar spacing, which exhibits that $Ce(NO_3)_3$/PVP has a certain degree of crystallinity. This result shows that the presence of $Ce(NO_3)_3$ exerts an influence on the crystallinity of PVP, and there might be some interaction between $Ce(NO_3)_3$ molecules and PVP.[10]

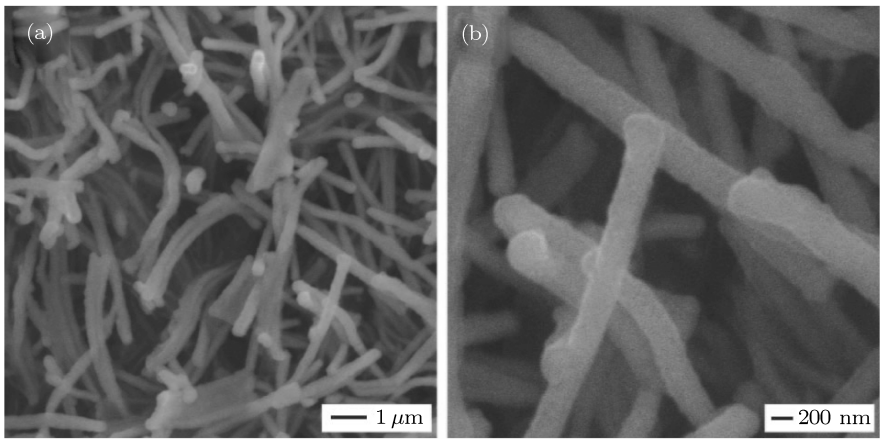


Fig. 4. SEM images of resulting CeO_2 nanowires obtained by calcining $Ce(NO_3)_3$/PVP composite fibres at 500 °C for 3 h.

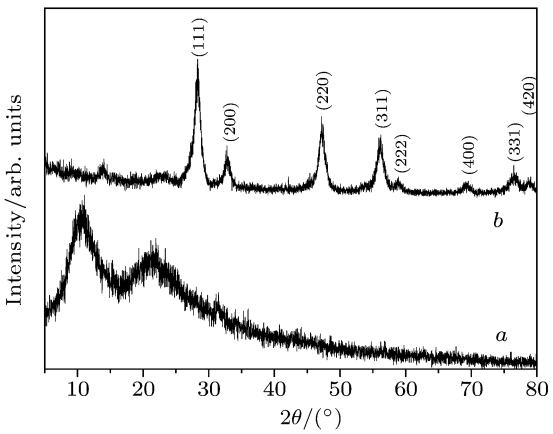


Fig. 5. XRD patterns of curve *a* $Ce(NO_3)_3$/PVP composite fibres and curve *b* CeO_2 nanowires.

The characteristic pattern of calcined products is shown in curve *b* and the main peaks can be indexed to the cerium oxide phase (JCPDS, card no. 43-1002). These results suggest the formation of pure CeO_2 nanowires after calcinations.

3.3. Fluorescent properties

The room temperature emission spectra of $Ce(NO_3)_3$/PVP composite fibres and CeO_2 nanowires monitored at the excitation wavelength of 321 nm are illustrated in Fig. 6. Curves *a*, *b* and *c* represent the emissions of composite fibres with 0.47 wt%, 0.92 wt%, and 1.38 wt% $Ce(NO_3)_3$, respectively. Curve *d* represents the photoluminescence (PL) of the resulting CeO_2 nanowires and the spectrum of analytical grade CeO_2 (curve *e*) is measured as reference. For the

composite fibres with different amounts of $Ce(NO_3)_3$, there is no particular shift of the PL peak position, with an apparent band around 371 nm. It can be concluded that the fluorescence properties of composite fibres are independent of concentration of $Ce(NO_3)_3$, which is different from the case of dyes.[31] As for the emission spectra of the resulting CeO_2 nanowires, it is observed that the band shifts to 384 nm in comparison with electrospun fibres, which is similar to that of analytical grade CeO_2.

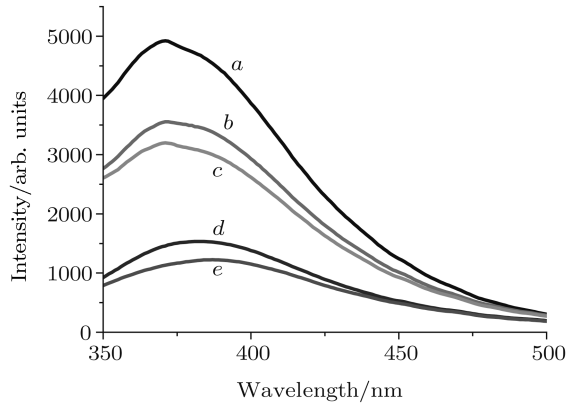


Fig. 6. Emission spectra of electrospun composite fibres with different amounts of $Ce(NO_3)_3$ (curves *a*, *b*, and *c* are for 0.47 wt%, 0.92 wt%, and 1.38 wt%, respectively) and CeO_2 (curve *d* is the resulting nanowires by calcining composite fibres, and curve *e* is the analytical grade).

3.4. Fibre-division model

It is interesting that we have observed ribbon-like or twin fibres besides the usual circular fibres. They are like anaphase and/or telophase states of the cell division as shown in Figs. 2 and 6. Similar ribbons have been observed in electrospun hydroxypropyl methyl cellulose phthalate/erythromycin fibres,[26] poly(L-lactic acid) fibres,[27] carbon fibres[22,23] and zein fibres.[32] Here it should be noted that our observed ribbons or twin fibres are slightly different from the flat ribbons reported by Koombhongse *et al.*[21,22,28,29] The ribbons mainly show that their surfaces are very smooth and not wrinkled. In addition, many long ribbons exhibit twin-fibre structures with cocoon-like shapes. As demonstrated previously by Koombhongse *et al.*,[21] collapsing from a thin walled tube formed on the moving liquid jet due to a rapid vaporization of solvent from the surface of the jet may be one of the possible reasons for the formation of such ribbon structures. However, the formation of the thin walled tube is questionable for the present case and some other cases.[20,21,26,27] In addition, splitting resulting from Coulomb repulsion of the charges on the skin of the jet may be also a key reason.[22]

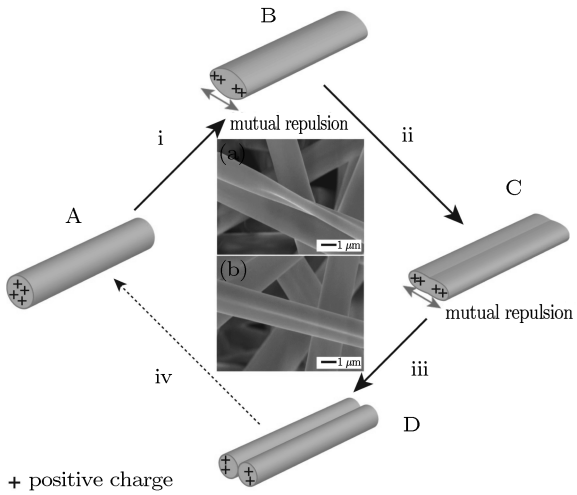


Fig. 7. Schematic of the fibre-division model and SEM images of (a) electrospun fibres deformed from state B (elliptic shape) to state C (ribbon-like shape) and (b) the ribbon-like fibres.

As we know, when electric forces overcome the surface tension forces, the charged polymer jets are ejected from the Taylor cone, carrying a large number of positive charges due to the applied high dc voltage, and then rush towards the collector. The fibres become increasingly thinner because of elongation and/or splitting in the process of electrospinning. In addition, it is less possible that the twin-fibre-like ribbons are formed by combing two individual spun fibres because they carry the same positive charges and repulse each other. Here, based on our observed experimental results, we develop a fibre-division model resulting from Coulomb repulsion and solvent vaporization in order to interpret the formation of the ribbons. As shown in Fig. 7, in the whole process of electrospinning: (i) Under the actions of static electric field and mutual repulsion in the jet, as well as the influence of some kind of perturbation or instability,[17] positive charges could be disturbed and redistributed, and Coulomb repulsion begins to make the fibre/jet deformed and have an elliptic cross section (state B). Here it is worth while to note that an asymmetrical vaporization of solvent from the surface can also make the jet deformed, but it is less possible to be the main reason for deformation in this case due to the size of the fibre/jet. (ii) If Coulomb repulsion is strong enough, the repulsion forces may stretch the fibre from state B (elliptic shape) to state C (ribbon-like shape)

gradually, just like from metaphase to anaphase in cell mitosis. From Fig. 7(a), it can be clearly observed that a shallow gap along fibre axis appears on the surface of the fibre. (iii) As the fibre-division continues, the gap becomes deeper and fibre segments on both sides of the gap tend to be of a cylindrical shape (state D). Herein we define fibres with states between C and D as ribbon-like fibres or twin-fibre-like ribbons. (iv) When the Coulomb repulsion surpasses the viscous force and surface tension, two new fibres are produced from a ribbon-like fibre, each with a smaller diameter than that of parent fibre. If the Coulomb repulsion force, the viscous force and the surface tension cannot reach a balance, a further fibre division will occur and continue until the jets are deposited on the collector.

In this study, the $Ce(NO_3)_3$/PVP precursor solutions with different $Ce(NO_3)_3$ loadings were used to spin in the same experimental conditions. With the loading of $Ce(NO_3)_3$ increasing, the viscosity of spun solution is increased and there are more ions in the solution, so that viscous force and Coulomb repulsion are enhanced efficiently. Whereas, it is found that the viscosity is a more important factor than the increased ions during the electrospinning process. A higher viscosity can slow down the fibre division and prolong the division period. As a result, when $Ce(NO_3)_3$ content increases, there will be fewer fibre divisions and an enhancement of fibres diameter. This analysis is consistent with the results of Figs. 2(a)–2(c).

3.5. Influence of operation voltage and work distance

Since Rojas *et al.*[25] proposed that the relatively high voltage used in electrospinning favoured the formation of ribbons, we have further studied the influence of experimental parameters on the formation of the ribbon-like fibres. One group of experiments was to fix the work distance (15 cm) and set the operation voltages to be 15, 20, and 25 kV, separately. In another one, the applied dc voltage was fixed to be 20 kV and the work distance was varied from 12 cm to 15 and 18 cm separately. The SEM images in Figs. 8 and 9 exhibit that ribbons or twin fibres are observed in all these cases. It is known that the applied dc voltage and the work distance can change the strength of electric field and thus the electric forces on the charged jet/fibre. Previous results have shown that the morphologies of spun fibres can be modified by changing voltage or work distance.[11] However, the above results indicate that the formation of ribbon-like fibre is less dependent on applied voltage and work distance.

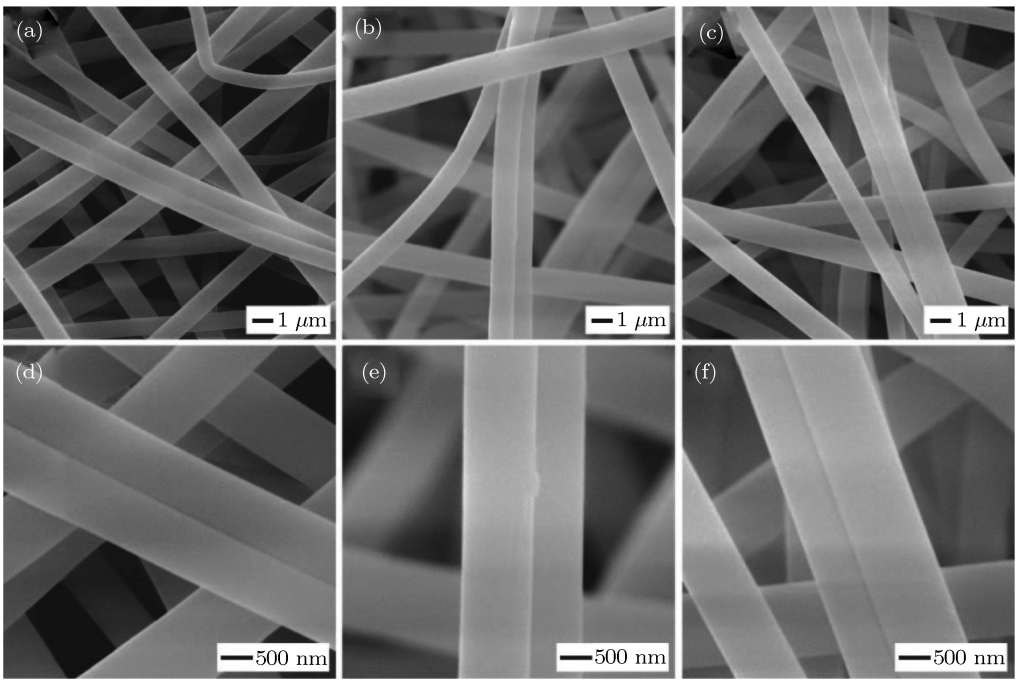


Fig. 8. SEM images of composite fibres in the presence of different applied high voltages. (a)–(c) Applied high voltages are 15, 20, and 25 kV, respectively. (d)–(f) Typical enlarged SEM images of panels (a)–(c). Ribbon-like or twin fibres are observed in these cases.

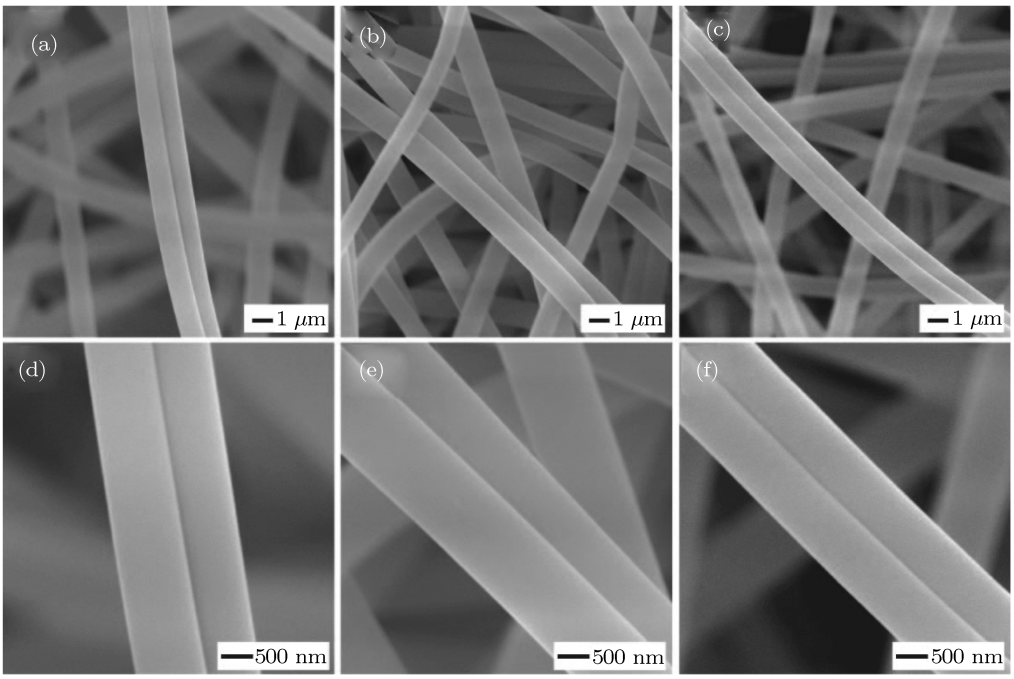


Fig. 9. SEM images of composite fibres in the presence of different work distances. Work distances are (a) 12, (b) 15, and (c) 18 cm. Panels (d)–(f) show typical enlarged SEM image of panels (a)–(c). Ribbon-like or twin fibres are also observed.

The possible reason is that the fibre division is mainly related to an inner mechanical equilibrium of the charged fibre, which depends on physical properties (e.g., viscosity and electrical conductivity) of precursor solution.[17,22,29]

4. Conclusion

Cerium nitrate/polymer (with 0.47, 0.92 and 1.38 wt% $Ce(NO_3)_3$) composite fibres are fabricated by electrospinning. After calcination, 200-nm CeO_2 nanowires are also successfully obtained. Their morphological, structural and fluorescent properties are characterized. It is interesting that unusual ribbon-like or twin fibres are observed. A fibre-division model resulting from Coulomb repulsion and solvent vaporization is developed to explain the formation of the ribbons or twin fibres. This model is confirmed by SEM studies. It is found that the formation of the ribbons or twin fibres is less dependent on operation voltage and work distance. Further studies on the mechanism of formation of the ribbons or twin fibres are still needed.

References

[1] Atanassov G, Thielsch R and Popov D 1993 *Thin Solid Films* **223** 288
[2] Netterfield R P, Sainty W G, Martin P J and Sie S H 1985 *Appl. Opt.* **24** 2267
[3] Norton D P, Budai J D and Chilsom M F 2000 *Appl. Phys. Lett.* **76** 1677
[4] Zhang Z L, Du X H and Wang W D 2000 *J. Vac. Sci. Technol.* A **18** 2928
[5] Zhou X D, Huebner W and Anderson H U 2003 *Chem. Mater.* **15** 378
[6] Zhou X D and Huebner W 2002 *Appl. Phys. Lett.* **80** 3814
[7] Zhou X D, Huebner W and Aderson H U 2001 *Appl. Phys. Lett.* **79** 3512
[8] Tsunekawa S, Fukuda T and Kasuya A 2000 *J. Appl. Phys.* **87** 1318
[9] Wang H, Zhu J J, Zhu J M, Liao X H, Xu S, Ding T and Chen H Y 2002 *Phys. Chem. Chem. Phys.* **4** 3794
[10] Yang X G, Shao C L, Liu Y C, Mu R X and Guan H Y 2005 *Thin Solid Films* **478** 228
[11] Huang Z M, Zhang Y Z, Kotaki M and Ramakrishna S 2003 *Compos. Sci. Technol.* **63** 2223
[12] Li M M, Long Y Z, Tan J S, Yin H X, Sui W M and Zhang Z M 2010 *Chin. Phys.* B **19** 028102
[13] Tan J S, Long Y Z and Li M M 2008 *Chin. Phys. Lett.* **25** 3067
[14] Xiang J, Shen X Q, Song F Z and Liu M Q 2009 *Chin. Phys.* B **18** 4960

[15] Li M M, Yang D Y, Long Y Z and Ma H W 2010 *Nanoscale* **2** 218

[16] Greiner A and Wendorff J H 2008 *Adv. Polym. Sci.* **219** 107

[17] Reneker D H and Yarin A L 2008 *Polymer* **49** 2387

[18] Schiffman J D and Schauer C L 2008 *Polymer Rev.* **48** 317

[19] Agarwal S, Wendorff J H and Greiner A 2008 *Polymer* **49** 5603

[20] Huang L, McMillan R A, Apkarian R P, Pourdeyhimi B, Conticello V P and Chaikof E L 2000 *Macromolecules* **33** 2989

[21] Koombhongse S, Liu W and Reneker D H 2001 *J. Polym. Sci.* B: *Polym. Phys.* **39** 2598

[22] Park S H, Kim C, Choi Y O and Yang K S 2003 *Carbon* **41** 2653

[23] Park S H, Kim C, Jeong Y I, Lim D Y, Lee Y E and Yang K S 2004 *Synth. Metals* **146** 207

[24] McCann J T, Chen J I L, Li D, Ye Z G and Xia Y N 2006 *Chem. Phys. Lett.* **424** 162

[25] Rojas O J, Montero G A and Habibi Y 2009 *J. Appl. Polym. Sci.* **113** 927

[26] Wang M, Wang L and Huang Y 2007 *J. Appl. Polym. Sci.* **106** 2177

[27] Zeng J, Xu X Y, Chen X S, Liang Q Z, Bian X C, Yang L X and Jing X B 2003 *J. Control Release* **92** 227

[28] Huang C B, Chen S L, Lai C L, Reneker D H, Qiu H Y, Ye Y and Hou H Q 2006 *Nanotechnology* **17** 1558

[29] Tao J and Shivkumar S 2007 *Mater. Lett.* **61** 2325

[30] Zhang H, Song H W, Dong B, Han L L, Pan G H, Bai X, Fan L, Lu S Z, Zhao H F and Wang F 2008 *J. Phys. Chem.* C **112** 9155

[31] Yan E, Huang Z H, Xin Y, Zhao Q and Zhang W 2006 *Mater. Lett.* **60** 2969

[32] Selling G W, Woods K K, Sessa D and Biswas A 2008 *Macromol. Chem. Phys.* **209** 1003